

# The study of gluon energy loss in cold nuclear matter from $J/\psi$ production<sup>\*</sup>

Li-Hua Song(宋丽华)<sup>1)</sup> Lin-Wan Yan(闫琳婉) Shang-Fei Xin(辛尚菲)

College of Science, North China University of Science and Technology, Tangshan 063210, China

**Abstract:** The energy loss effects of the incident quark, gluon, and the color octet  $c\bar{c}$  on  $J/\psi$  suppression in p-A collisions are studied by means of the experimental data at E866, RHIC, and LHC energy. We extracted the transport coefficient for gluon energy loss from the E866 experimental data in the middle  $x_F$  region ( $0.20 < x_F < 0.65$ ) based on the Salgado-Wiedemann (SW) quenching weights and the recent EPPS16 nuclear parton distribution functions together with nCTEQ15. It was determined that the difference between the values of the transport coefficient for light quark, gluon, and heavy quark in cold nuclear matter is very small. The theoretical results modified by the parton energy loss effects are consistent with the experimental data for E866 and RHIC energy, and the gluon energy loss plays a remarkable role on  $J/\psi$  suppression in a broad variable range. Because the corrections of the nuclear parton distribution functions in the  $J/\psi$  channel are significant at LHC energy level, the nuclear modification due to the parton energy loss is minimal. It is worth noting that we use the color evaporation model (CEM) at leading order to compute the p-p baseline, and the conclusion in this paper is CEM model dependent.

**Keywords:**  $J/\psi$  production, energy loss, charm quark, gluon

**PACS:** 24.85.+p, 25.40.-h, 12.38.-t **DOI:** 10.1088/1674-1137/42/12/124103

## 1 Introduction

In the past thirty years, the study of the origin of  $J/\psi$  suppression in p-A collisions has become important for the understanding of the Quark-Gluon Plasma (QGP), the state of matter where quarks and gluons are deconfined. Due to the Debye color screening of the charm-quark potential, the high quark density in the QGP formation could suppress the yield of  $J/\psi$  mesons in high-energy heavy-ion collisions relative to that in p-p collisions [1]. The generic features of hard quantum chromodynamics (QCD) processes in the nuclear environment can be quantified based on experimental data of  $J/\psi$  production in p-A collisions. This can assist in the process of reliable baseline predictions of the properties of the QGP formed in heavy-ion collisions.

In  $J/\psi$  production from p-A collisions, the charmonium production can be modified by cold nuclear matter effects, such as parton energy loss [2], nuclear absorption, and modification of the parton distribution functions due to the nuclear environment [3]. It is necessary to constrain the so-called cold nuclear matter effects for quarkonium production to unambiguously in-

terpret these results in heavy-ion collisions. The wealth of available data on p-A collisions from a wide collision energy range (e.g., NA3 [4], E772 [5], E866 [6, 7], NA50 [8], HEAR-B [9], LHC [10, 11], and RHIC [12]) results in insightful probes on the origin of  $J/\psi$  suppression. However, the conventional nuclear suppression mechanism of  $J/\psi$  is still an open question, owing to the presence of various competing effects, depending on the precise kinematics and collision energy. Currently, a few phenomenological approaches are being proposed on the basis of hadron nuclear absorption or the shadowing of gluon distribution for the target nucleus expected in the small  $x_2$  range ( $x_2 < 10^{-2}$ ). In addition, another fundamental phenomenological model assumes that the parton energy loss induced by parton multiple scattering in the nuclear environment plays a decisive role in  $J/\psi$  suppression [13].

Because the intensity of each cold nuclear matter effect is usually unknown, a priori, it is a viable strategy to investigate each of these effects separately by comparing all available data systematically and quantitatively, while maintaining the minimum number of assumptions and free parameters. We find it interesting that the mod-

Received 4 June 2018, Revised 11 August 2018, Published online 25 October 2018

<sup>\*</sup> Supported by National Natural Science Foundation of China (11405043) and Natural Science Foundation of Hebei Province (A2018209269)

1) E-mail: songlh@ncst.edu.cn



Content from this work may be used under the terms of the Creative Commons Attribution 3.0 license. Any further distribution of this work must maintain attribution to the author(s) and the title of the work, journal citation and DOI. Article funded by SCOAP<sup>3</sup> and published under license by Chinese Physical Society and the Institute of High Energy Physics of the Chinese Academy of Sciences and the Institute of Modern Physics of the Chinese Academy of Sciences and IOP Publishing Ltd

ified parton distribution functions and parton energy loss effect can describe the  $J/\psi$  suppression measured in p-A collisions when a high-energy  $J/\psi$  is formed long after the nucleus. Consequently, following our previous work on the parton energy loss effect in cold nuclear matter [14-16], we present a phenomenological approach based on the assumption that the observed  $J/\psi$  suppression is mainly induced by nuclear PDF effects and the energy loss effects of incoming quarks, gluons, and the color octets  $c\bar{c}$ . By utilizing the Salgado-Wiedemann (SW) quenching weights [17], we will separately investigate the incident quark energy loss, the incident gluon energy loss, and the color octet  $c\bar{c}$  energy loss by comparing the E866 [6, 7], LHC [10, 11], and RHIC [12] experimental data. As the strength of each parton energy loss depends on a single free parameter (called the transport coefficient), which characterizes the medium-induced transverse momentum squared transferred to the projectile per unit path length, this research may contribute to the understanding of the microscopic dynamics of medium-induced parton energy loss, corresponding to the color charge of the parton.

The remainder of this article is arranged as follows. The theoretical framework of our study is introduced in Section II, and the results for the nuclear modification of  $J/\psi$  production on the basis of the nuclear PDF effects and parton energy loss effect are given in Sections III. We then summarize our main conclusions in Section IV.

## 2 $J/\psi$ production modified due to energy loss effect

In  $J/\psi$  production from p-A collisions, a hard parton traveling through a nuclear target undergoes multiple soft collisions which induce gluon emission. Medium-induced gluon radiation modifies the correspondence between the initial parton and the final hadron momenta. Based on the assumption that these radiated gluons take away energy  $\varepsilon$  from the leading particle, this modification is determined by the probability distribution  $D(\varepsilon)$  associated with the energy loss. If gluons are emitted independently,  $D(\varepsilon)$  is the normalized sum of the emission probabilities for an arbitrary number of  $n$  gluons that carry away the total energy  $\varepsilon$  [17]:

$$D(\varepsilon) = \sum_{n=0}^{\infty} \frac{1}{n!} \left[ \prod_{i=1}^n \int d\omega_i \frac{dI(\omega_i)}{d\omega} \right] \delta \left( \varepsilon - \sum_{i=1}^n \omega_i \right) \times \exp \left[ - \int_0^{+\infty} d\omega \frac{dI(\omega)}{d\omega} \right]. \quad (1)$$

Here,  $dI(\omega)/d\omega$  is the medium-induced gluon spectrum. According to Ref. [18], the probability distribution  $D(\varepsilon)$  has a discrete and a continuous part:

$$D(\varepsilon) = p_0 \delta(\varepsilon) + p(\varepsilon). \quad (2)$$

Its normalization is unity. In this paper, the probability distribution  $D(\varepsilon)$  that is used is calculated in the multiple soft and single hard scattering approximations, and the results termed as SW quenching weights are available as a FORTRAN routine [19]. The SW quenching weight is a scaling function of the variables  $\varepsilon/E$  and  $\varepsilon/\omega_c$ , where  $E$  represents the parton energy after radiating the energy  $\varepsilon$  and  $\omega_c = \frac{1}{2} \hat{q} L^2$ . Here,  $\hat{q}$  denotes the transport coefficient and  $L$  is the path length covered by the parton in the nuclear medium. In general, the cross-section in the medium can be modified as:

$$\sigma^{\text{medium}} = D(\varepsilon) \otimes \sigma^{\text{vacuum}}. \quad (3)$$

Then, the charmonium production cross-section  $d\sigma_{p-A}/dx_F$  can be expressed as:

$$\frac{d\sigma_{p-A}}{dx_F}(x_F) = \int_0^{\varepsilon_{\text{max}}} d\varepsilon D(\varepsilon) \frac{d\sigma_{p-p}}{dx_F}(\varepsilon, x_F), \quad (4)$$

where the upper limit on the energy loss is  $\varepsilon_{\text{max}} = \min(E_p - E, E)$  where  $E_p$  denotes the beam energy in the rest frame of the target nucleus.

This medium-induced energy loss leads to the rescaling of the parton momentum fraction. In view of the energy loss effect of the color octet  $c\bar{c}$  pair, the observed  $J/\psi$  at a given  $x_F$  actually comes from a  $c\bar{c}$  pair originally produced at the higher value  $x'_F = x_F + \Delta x_F$  where  $\Delta x_F = \varepsilon_{c\bar{c}}/E_p$ . The energy loss of the incoming gluon (quark) also results in a change in its momentum fraction prior to the collision:  $\Delta x_{1g} = \varepsilon_g/E_p$  ( $\Delta x_{1q} = \varepsilon_q/E_p$ ). In order to incorporate the features of the process for  $J/\psi$  production, two acceptable formalisms have been presented; the non-relativistic QCD (NRQCD) [20] and the color evaporation model (CEM) [21]. These models have been proven to be successful in accounting for charmonium phenomenology. In this work, we chose the CEM as it has fewer free parameters [22-26]. Based on the CEM [21] and considering the aforementioned rescaling, the cross-section  $d\sigma_{p-p}/dx_F$  (a convolution of the  $q\bar{q}$  cross-section ( $\sigma_{q\bar{q}}$ ) and  $gg$  cross-section ( $\sigma_{gg}$ ) with the parton distribution functions  $f_i$  in the incident proton and  $f_i^A$  in the target proton) can be expressed as:

$$\begin{aligned} \frac{d\sigma_{p-p}}{dx_F}(x_F, \varepsilon_{c\bar{c}, g, q}) &= \rho_{J/\psi} \int_{2m_c}^{2m_D} dm \frac{2m}{\sqrt{x_F^2 s + 4m^2}} \\ &\times [f_g(x'_{1g}, m^2) f_g^A(x'_{2g}, m^2) \sigma_{gg}(m^2) \\ &+ \sum_{q=u, d, s} \{f_q(x'_{1q}, m^2) f_q^A(x'_{2q}, m^2) \\ &+ f_{\bar{q}}(x'_{1q}, m^2) f_{\bar{q}}^A(x'_{2q}, m^2)\} \sigma_{q\bar{q}}(m^2)], \end{aligned} \quad (5)$$

where  $x'_{1g(q)} = x'_1 + \Delta x_{1g(q)}$ ,

$$x'_1 = \frac{1}{2} [\sqrt{(x'_F)^2 (1 - m^2/s)^2 + 4m^2/s} + x'_F (1 - m^2/s)],$$

$m^2 = x_1 x_2 s$  in the rest frame of the target nuclei, and  $\rho_{J/\psi}$  denotes the fraction of the  $c\bar{c}$  pair evolving into the

$J/\psi$  state. It is indicated that the following calculation is based on the leading order in CEM, especially on the solutions of the momentum fractions.

Analogously, owing to the energy loss effects, the

charmonium production cross section as a function of the rapidity  $y$  (with  $x_{1(2)} = \frac{m}{\sqrt{s}}e^{\pm y}$  and  $E = E_p e^y m/\sqrt{s}$ ) can be modified as:

$$\begin{aligned} \frac{d\sigma_{p-p}}{dy}(y) = & \rho_{J/\psi} \int_{2m_c}^{2m_D} dm \frac{2m}{s} \times [f_g(x'_{1g}, m^2) f_g^A(x'_{2g}, m^2) \sigma_{gg}(m^2) \\ & + \sum_{q=u,d,s} \{f_q(x'_{1q}, m^2) f_{\bar{q}}^A(x'_{2q}, m^2) + f_{\bar{q}}(x'_{1q}, m^2) f_q^A(x'_{2q}, m^2)\} \sigma_{q\bar{q}}(m^2)]. \end{aligned} \quad (6)$$

Here,  $x'_{1g(q)} = \frac{m}{\sqrt{s}}e^{y'} + \Delta x_{1g(q)}$  and  $y' = y + \ln(\frac{E + \varepsilon_{c\bar{c}}}{E})$ .

### 3 Results and discussion

The amount of medium-induced gluon radiation and the strength of the  $J/\psi$  suppression in p-A collisions are controlled by the transport coefficient  $\hat{q}$  in the target nucleus. Based on the preceding parton energy loss model expressed in Section 2, we can extract the transport coefficient  $\hat{q}_g$  for the gluon energy loss from the E866 experimental data [6, 7] using the SW quenching weights for gluons [17]. It is worth noting that according to Ref. [27] the  $c\bar{c}$  remains colored on its entire path for the E866 energy ( $\sqrt{s} = 38.7$  GeV) in the range  $0.20 \leq x_F \leq 0.65$ . The extracted results of the transport coefficient  $\hat{q}_g$  are summarized in Table 1, using the CERN subroutine MINUIT [28] and the recent EPPS16 nuclear parton distributions [29] together with nCTEQ15 parton density in the proton bound in a nucleus [30]. In this calculation, we employed the values of the path  $L$  obtained from the Glauber model calculation using realistic nuclear densities [31],  $\hat{q}_q = 0.32 \pm 0.04$  GeV<sup>2</sup>/fm extracted from the nuclear Drell-Yan experimental data using the SW quenching weights, for light quarks [15], and  $\hat{q}_{c\bar{c}} = 0.29 \pm 0.07$  GeV<sup>2</sup>/fm obtained using the SW quenching weights for heavy quarks [32].

From Table 1, it can be observed that the theoretical results are in good agreement with the E866 experimental data in the  $0.20 < x_F < 0.65$  range ( $\chi^2/ndf = 1.10$ ). The experimental data including the small and large  $x_F$  regions deviate from the calculated results ( $\chi^2/ndf = 23.19$ ), which illustrates that the influence of other nuclear effects (such as gluon saturation at small  $x_F$  region and nuclear absorption at big  $x_F$  region) on the modification of the charmonium production cross-section cannot be ignored in the small or big  $x_F$  range. Consequently, we determined the transport coefficient  $\hat{q}_g$  ( $\hat{q}_g = 0.31 \pm 0.02$  GeV<sup>2</sup>/fm) for the gluon energy loss from the data in the middle region  $0.20 < x_F < 0.65$ . It is determined that the difference between these values for the transport coefficient for light quark, gluon, and heavy quark in cold nuclear matter is very small. This conclusion contradicts the well-known statement that the transport coefficient

$\hat{q}_g$  is larger than that of the quark owing to the ratio of the Casimir factors  $C_A/C_F = 9/4$  in the leading logarithmic approximation. It is worth emphasizing that the obtained energy loss for an incoming quark based on the Drell-Yan experimental data depends strongly on the nuclear parton distribution functions (see Ref. [33] for a detailed discussion). The recent EPPS16 nuclear parton distributions provide the uncertainty estimates are more objective flavor by flavor [29]. The errors of  $\hat{q}_g$  from the uncertainty of the nuclear PDFs EPPS16 were analyzed. The extracted value of  $\hat{q}_g$  for the specific error sets  $S_1^-$  ( $S_1^+$ ) for EPPS16 is  $\hat{q}_g = 0.30 \pm 0.02$  GeV<sup>2</sup>/fm ( $\hat{q}_g = 0.32 \pm 0.02$  GeV<sup>2</sup>/fm). In addition, the nuclear modification for the gluon distribution function is apparently different between the different sets, as discussed in Ref. [34]. The uncertainty of the gluon distribution function may be the main source of the uncertainty associated with the result of the transport coefficient  $\hat{q}_g$ . To further examine the initial state PDFs' dependence on the determination of the jet transport coefficient, we simply eliminate the nuclear dependence of the PDFs by using the nCTEQ15 parton density, the transport coefficient  $\hat{q}_g = 0.35 \pm 0.03$  GeV<sup>2</sup>/fm extracted from the E866 experimental data for the range  $0.20 < x_F < 0.65$ .

Table 1. The values of  $\hat{q}_g$  and  $\chi^2/ndf$  extracted from the E866 experimental data [6, 7].

$x_F$	No.data	$\hat{q}/(\text{GeV}^2/\text{fm})$	$\chi^2/ndf$
$0.20 < x_F < 0.65$	18	$0.31 \pm 0.02$	1.10
$0.30 < x_F < 0.95$	26	$0.26 \pm 0.01$	15.41
$0.20 < x_F < 0.95$	44	$0.26 \pm 0.01$	10.29
$0.00 < x_F < 0.95$	49	$0.25 \pm 0.01$	23.19

In Fig. 1, with  $\hat{q}_g = 0.31 \pm 0.02$  GeV<sup>2</sup>/fm,  $\hat{q}_q = 0.32 \pm 0.04$  GeV<sup>2</sup>/fm, and  $\hat{q}_{c\bar{c}} = 0.29 \pm 0.07$  GeV<sup>2</sup>/fm, we initially compare the model predictions with the E866 data for  $J/\psi$  production in the range  $0.20 < x_F < 0.65$ . The solid lines denote the results modified only by the EPPS16 nuclear parton distributions, the dashed curves represent the calculations including the incident quark energy loss in the initial state and the  $c\bar{c}$  energy loss in the final state, and the dotted lines represent the results with the incident gluon energy loss correction.

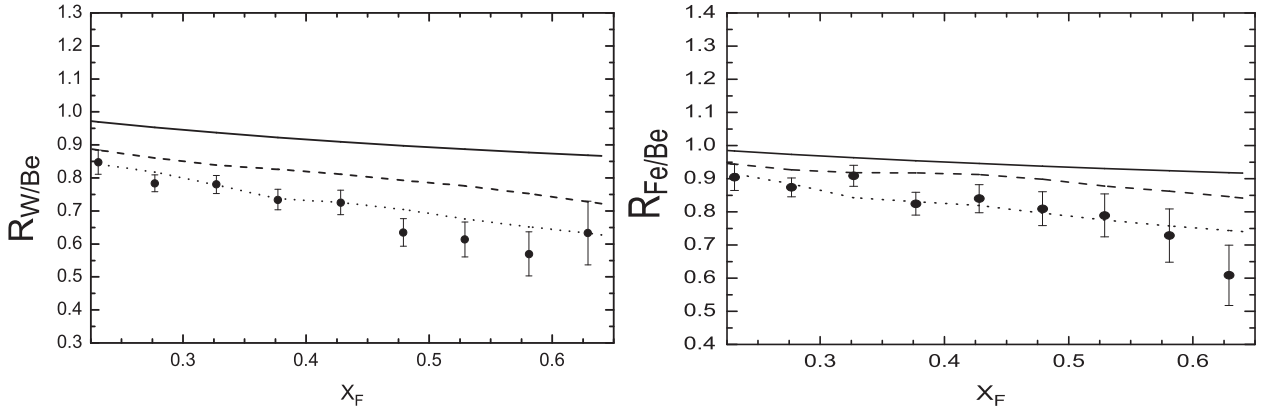


Fig. 1. The  $J/\psi$  production cross-section ratios  $R_{W(\text{Fe})/\text{Be}}(x_F)$  for  $0.20 < x_F < 0.65$ . The solid lines denote the results modified only by the EPPS16 nuclear parton distributions, the dashed curves represent the calculations including the incident quark energy loss in the initial state and the  $c\bar{c}$  energy loss in the final state, and the dotted lines represent the results with the incident gluon energy loss correction. The experimental points are taken from the E866 data for  $J/\psi$  production in p-A collisions [6, 7].

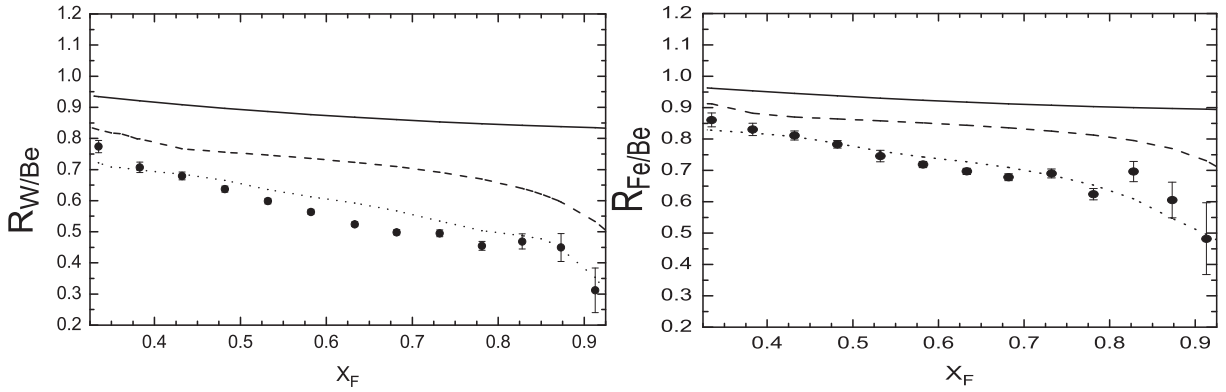


Fig. 2. The  $J/\psi$  production cross-section ratios  $R_{W(\text{Fe})/\text{Be}}(x_F)$  for  $0.3 < x_F < 0.95$ . The dashed curves represent the calculations with the  $c\bar{c}$  energy loss. Other notations are the same as those in Fig. 1.

The good agreement as indicated by the dotted lines in Fig. 1 fully supports this energy loss model with the energy loss probability distribution calculated using SW quenching weights. From Fig. 1, it is also remarkable that the energy loss of the incident gluon in the initial state plays a certain role in  $J/\psi$  suppression. This indicates that the E866 data for  $J/\psi$  production in the range  $0.20 < x_F < 0.65$  would provide a good way to identify the gluon energy loss with a high degree of discrimination. In Fig. 2, the calculated results are also compared with the E866 data for  $0.30 < x_F < 0.95$ . The strength of the  $J/\psi$  suppression induced by the  $c\bar{c}$  energy loss effect is shown as dashed lines in Fig. 2, which indicates that the nuclear modification due to the  $c\bar{c}$  energy loss is more significant at larger targets for larger  $x_F$  regions. From Fig. 2, we can also observe that the predictions of the dotted lines (including the correction induced by the quark, gluon, and  $c\bar{c}$  energy loss) are consistent with the experimental data for  $0.30 < x_F < 0.95$ . From the solid lines in Fig. 1 and Fig. 2, we can see that nuclear sup-

pression from the nuclear modification of the EPPS16 nuclear parton distributions becomes larger with the increase of  $x_F$  in the range  $0.20 < x_F < 0.95$ . The nucleon parton momentum fractions  $x_2$  is  $1.84 \times 10^{-2}$  to  $4.22 \times 10^{-3}$  accordance to the  $x_F$  range from 0.20 to 0.95. In this  $x_2$  range, the shadowing effect plays an important role. The suppression induced by the shadowing effect of the nuclear parton distributions increases with the decrease of  $x_2$ . The dashed and dotted lines in Fig. 1 and Fig. 2 indicate that the suppression due to the  $c\bar{c}$  and incoming gluon energy loss also becomes larger with the increase of  $x_F$  in the range  $0.20 < x_F < 0.95$ .

Furthermore, we discuss the  $J/\psi$  suppression expected for d-Au collisions at the RHIC ( $\sqrt{s} = 200$  GeV) [12] and for p-Pb collisions at the LHC ( $\sqrt{s} = 5.0$  TeV) [10, 11]. The comparisons between the RHIC data and the proposed model predictions are shown in Fig. 3. The solid lines denote the results modified only by the EPPS16 nuclear parton distributions, the dashed curves represent the calculations including the incident quark

energy loss in the initial state and the  $c\bar{c}$  energy loss in the final state, and the dotted lines represent the results with the incident gluon energy loss correction. As can be seen from Fig. 3, the energy loss model is able to reproduce the  $J/\psi$  suppression over the entire variable interval. It is worth noting that a good agreement is also observed in some negative  $y$  bins for  $y < y^{\text{crit}}$  ( $y^{\text{crit}} = -1.1$ ), where nuclear absorption might also play a role. In addition, the prediction of the dotted line illustrates that the gluon energy loss can induce the obvious suppression of  $J/\psi$  production in a broad  $y$  range. In Fig. 3, the tendency of the solid line modified only by the EPPS16 nuclear parton distribution shows an enhancement in the range  $-2.1 < y < -1.5$ , then falls with the increase of  $y$  in the range  $-1.5 < y < 2.4$ . The physical reasons for the  $y$  dependence of the nuclear modification from the EPPS16 densities are that the anti-shadowing effect induces the enhancement in the coverage  $-2.0 < y < -1.5$  ( $0.09 > x_2 > 0.05$ ), and the shadowing effect causes a suppression for  $-1.5 < y < 2.4$  ( $0.05 > x_2 > 0.001$ ). The parton energy loss effects have the analogous tendency as the increase of  $y$  in the range  $-2.1 < y < 2.4$ .

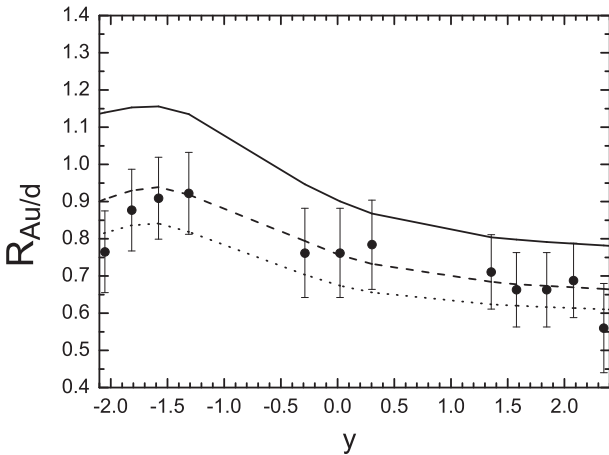


Fig. 3. The  $J/\psi$  production cross-section ratio  $R_{\text{Au}/d}(y)$ . The experimental points are taken from RHIC experimental data [12]. Other notations are the same as those in Fig. 1.

In Fig. 4, we separately show the  $J/\psi$  production cross-section ratio  $R_{\text{Pb}/p}(y)$ , modified only by the EPPS16 nuclear parton distribution (solid lines), only by  $c\bar{c}$  energy loss effect (dashed lines), only by the incident gluon energy loss (dotted lines), and only by the incident quark energy loss (dash-dot lines). From Fig. 4, we can see that the sole nuclear effects of the parton distribution might be responsible for the  $J/\psi$  observed suppression, and the nuclear modification due to the parton energy loss is minimal. This indicates that the corrections for the nuclear parton distribution functions in  $J/\psi$  production are significant for the high center-of-mass energy of

the collision at the LHC. In addition, it can be seen that the tendency of the nuclear modification of the EPPS16 distributions decreases steeply with the increase of  $y$  in the region  $-2.0 < y < -3.0$  and gradually in the region  $-3.0 < y < 3.5$ . For the LHC energy, the shadowing effect plays an important role in the range  $-2.0 < y < 3.5$  ( $0.04 > x_2 > 1.49 \times 10^{-5}$  and  $5.47 \times 10^{-6} < x_2 < 1.63 \times 10^{-2}$ ).

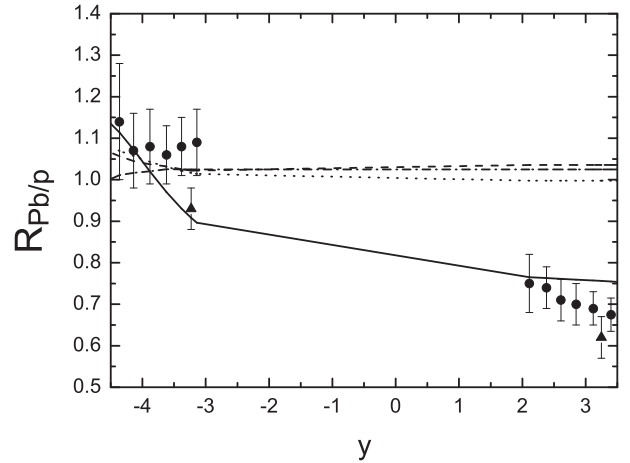


Fig. 4. The  $J/\psi$  production cross-section ratios  $R_{\text{Pb}/p}(y)$ , modified only by the EPPS16 nuclear parton distribution (solid lines), only by  $c\bar{c}$  energy loss effect (dashed lines), only by the incident gluon energy loss (dotted lines), and only by the incident quark energy loss (dash-dot lines). The experimental data are attributed to ALICE collaboration [10] (filled circles) and LHCb collaboration [11] (solid triangles).

## 4 Summary

Using the SW quenching weights and the recent EPPS16 nuclear parton distribution functions together with nCTEQ15, we investigate the energy loss effects of an incident quark, gluon, and color octet  $c\bar{c}$  on  $J/\psi$  suppression in p-A collisions. The transport coefficient  $\hat{q}_g$  ( $\hat{q}_g = 0.31 \pm 0.02 \text{ GeV}^2/\text{fm}$ , with  $\chi^2/\text{ndf} = 1.10$ ) for the gluon energy loss is extracted from the E866 data in the middle  $x_F$  region  $0.20 < x_F < 0.65$ . This indicates that the difference between the values of the transport coefficient for light quark ( $\hat{q}_q = 0.32 \pm 0.04 \text{ GeV}^2/\text{fm}$  [15]), gluon, and heavy quark ( $\hat{q}_{c\bar{c}} = 0.29 \pm 0.07 \text{ GeV}^2/\text{fm}$  [25]) in the cold nuclear matter, is very small. The good agreement between the proposed model with the E866 and RHIC experimental data strongly supports that the parton energy loss is a dominant effect in p-A quarkonium nuclear suppression when  $J/\psi$  formation occurs outside the nuclear target. It is also determined that the gluon energy loss in the initial state plays an important role in  $J/\psi$  suppression in a broad variable range at E866 and RHIC energies. However, the comparison between the

$J/\psi$  suppression data at LHC energy and our theoretical predictions indicate that the effects of the nuclear parton distribution functions are significant for the high center-of-mass energy of the collision at the LHC. In future work, it will be interesting to examine whether the L-dependence of the energy loss predicted in our present model is consistent with the centrality dependence of the

LHC data. It is worth noting that we use the CEM at the leading order to compute the p-p baseline, and the conclusion in this paper is CEM model dependent. We hope that this study on the parton energy loss effect on  $J/\psi$  production from p-A collisions will provide insight into the evaluation of  $J/\psi$  suppression in A-A collisions.

## References

- 1 T. Matsui and H. Satz, Phys. Lett. B, **178**: 416-422 (1986)
- 2 F. Arleo and S. Peigné, Journal of High Energy Physics, **3**: 122 (2013)
- 3 A. Andronic et al. Eur. Phys. J. C, **76**(3): 107, (2016)
- 4 J. Badier et al (NA3 Collaboration), Z. Phys. C, **20**: 101 (1983)
- 5 D. M. Alde et al (E772 Collaboration), Phys. Rev. Lett., **66**: 133 (1991)
- 6 M. J. Leitch et al (E866/NuSea Collaboration), Phys. Rev. Lett., **84**: 3256 (2000)
- 7 W. M. Lee, Ph.D. Thesis Georgia State University (1999)
- 8 B. Alessandro et al (NA50 Collaboration), Eur. Phys. J. C, **33**: 31 (2004)
- 9 I. Abt et al (HERA-B Collaboration), Eur. Phys. J. C, **60**: 525 (2009)
- 10 B. Abelev et al (ALICE Collaboration), JHEP, **1402**: 073 (2014)
- 11 R. Aaij et al (LHCb Collaboration), JHEP, **1402**: 072 (2014)
- 12 A. Adare et al (PHENIX Collaboration), Phys. Rev. Lett., **107**: 142301 (2011)
- 13 F. Arleo, S. Peigné, and T. Sami, Phys. Rev. D, **83**: 114036 (2011)
- 14 N. Liu, W. D. MIAO, L. H. Song, and C. G. Duan, Phys. Lett. B, **749**: 88-93 (2015)
- 15 L. H. Song and L. W. Yan, Phys. Rev. C, **96**: 045203 (2017)
- 16 L. H. Song and S. F. Xin, Journal of Physics G, **45**: 025005 (2018)
- 17 C. A. Salgado and U. A. Wiedemann, Phys. Rev. D, **68**: 014008 (2003)
- 18 C. A. Salgado and U. A. Wiedemann, Phys. Rev. Lett., **89**: 092303 (2002)
- 19 <http://www.aip.org/pubservs/epaps.html>
- 20 M. Kramer, Part. Nucl. Phys., **47**: 141 (2001)
- 21 H. Fritzsche, Phys. Lett. B, **67**: 217 (1977)
- 22 I. Abt et al, Eur. Phys. J. C, **60**: 517 (2009)
- 23 I. Abt et al, Eur. Phys. J. C, **49**: 545 (2007)
- 24 T. H. Chang et al, Phys. Rev. Lett., **91**: 211801 (2003)
- 25 R. Gavai et al, Int. J. Mod. Phys. A, **10**: 3043 (1995)
- 26 G. T. Bodwin et al, Phys. Rev. D, **72**: 014004 (2005)
- 27 D. Kharzeev and H. Z. Satz, Phys. C, **60**: 389 (1993)
- 28 James F CERN Program Library Long Writeup D506
- 29 K. J. Eskola et al, Eur. Phys. J. C, **77**: 163 (2017)
- 30 K. Kovarik et al, Phys. Rev. D, **93**: 085037 (2016)
- 31 F. Arleo and S. Peigné, JHEP, **03**: 122 (2013)
- 32 L. H. Song and L. W. Yan, Nuclear Physics A, NPA-D-18-00054 (2018)
- 33 C. G. Duan et al, Phys. Rev. C, **79**: 048201 (2009)
- 34 Chun-Gui Duan, Jian-Chao Xu, and Li-Hua Song, Eur. Phys. J. C, **67**: 173-179 (2010)